Vol 10 No 9, September 2001
1009-1963/2001/10(09)/0857-05
Chinese Physics
© 2001 Chin. Phys. Soc.
and IOP Publishing Ltd

THE STRUCTURE AND MAGNETIC PROPERTIES OF $La_{2-2x}Sr_1Ca_{2x}Mn_2O_7$ (x=0.25–1.00)

He Lun-hua(何伦华), Zhang Pan-lin(张泮霖), and Yan Qi-wei(严启伟)†

State Key Laboratory of Magnetism, Institute of Physics and Centre for Condensed Matter Physics, Chinese Academy of Sciences, Beijing 100080, *China*

(Received 29 April 2001; revised manuscript received 16 May 2001)

In this paper, the effect of divalent cation substitution on the structure and magnetic properties in $La_{2-2x}Sr_1Ca_{2x}Mn_2O_7$ have been investigated systematically using bulk samples with a wide doping concentration range $0.25 \leq x \leq 1.00$. Replacing trivalent La ions by divalent Ca ions results in the weakening and then disappearance of the long-range ferromagnetic (FM) ordering, the formation of spin canting, antiferromagnetic (AFM) ordering and low-temperature spin-glass. These results show that increasing the hole-doping concentration significantly suppresses the FM state. We suggest that this variation of magnetic properties is related to the competition of the FM and AFM interactions resulting from the change of Mn^{3+}/Mn^{4+} ratio and Jahn–Teller-type lattice distortion of MnO_6 octahedra due to the introduction of Ca^{2+} ions.

Keywords: structure, magnetic property
PACC: 7525, 7530, 7530E

I. INTRODUCTION

While the work on colossal magnetoresistance (CMR) materials has concentrated on the three-dimensional perovskites (e.g. $La_{1-x}Sr_xMnO_3$), the discovery of the layered materials of the formula $La_{2-2x}Sr_{1+2x}Mn_2O_7$, as another class of CMR oxide, has provided a rich opportunity to explore the interplay among the structure, magnetism and electronic transport in a reduced dimension.[1–6]

Previous studies have shown that the properties of the layered perovskites $Ln_{2-2x}M_{1+2x}Mn_2O_7$ (where Ln denotes lanthanide ions and M denotes divalent cations) are very sensitive to the element composition. In these systems, the trivalent Ln ions are substituted by divalent M ions leading to mixed valency of the transition metal ions (Mn^{3+}/Mn^{4+}). In a particular Mn^{3+}/Mn^{4+} ratio, the mixed valency leads to a strong ferromagnetic (FM) interaction arising from the Mn^{3+}-O-Mn^{4+} double-exchange (DE) mechanism,[7] which differs from the superexchange interaction that is usually antiferromagnetic (AFM). For $La_{2-2x}Sr_{1+2x}Mn_2O_7$,[2–5] when x=0.3 and 0.4, it is FM and metallic due to the DE interaction over the other interactions, but the FM and AFM phases coexist for x=0.5.

In addition to DE interactions, the lattice distortions play an important role through strong electron-lattice coupling which arises from the Jahn–Teller distortion around Mn^{3+} ions.[8] Chang *et al.*[9] found that, in the compounds $La_{1.4}(Sr_{1-x}Ca_x)_{1.6}Mn_2O_7$, the values of T_C and T_p decrease as the concentration of Ca increases from x=0.0 to 0.3. Ganguly *et al.*[10] investigated the magnetic properties of $La_{1.2}(Sr_{1-x}Ca_x)_{1.8}Mn_2O_7$ and found that, in the concentration region $0.0 \leq x \leq 0.5$, the value of T_C decreases with the increase of x, which can be explained on the basis of a decrease in the one-electron bandwidth of the e_g electrons due to Jahn–Teller distortion.

In this paper, we extend our study to the system of $La_{2-2x}Sr_1Ca_{2x}Mn_2O_7$ (x=0.25–1.00), investigating the variation of structural and magnetic properties.

II. EXPERIMENTAL DETAILS

Bulk samples of $La_{2-2x}Sr_1Ca_{2x}Mn_2O_7$ (x=0.25–1.00) were synthesized by a standard ceramic process. Stoichiometric amounts of La_2O_3, $CaCO_3$, $SrCO_3$ and $MnCO_3$ powders were mixed, ground, and calcined at 900°C for 24h in air with an intermediate grinding. The powder obtained was ground, pelletized, and sintered at 1370°C for 48h with an intermediate grinding. The samples were characterized by X-ray diffraction

†Corresponding author.

(XRD), and the crystal structures of some samples were refined from step-scanning XRD data using the Rietveld method. The magnetic measurements were performed on a SQUID magnetometer.

Ⅲ. RESULTS AND DISCUSSION

A. Structure

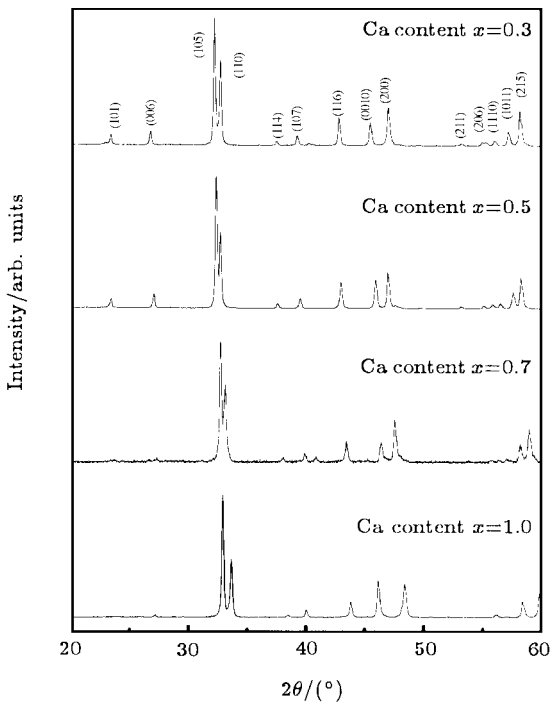


Fig.1. XRD patterns of the samples $La_{2-2x}Sr_1Ca_{2x}Mn_2O_7$ (x=0.3, 0.5, 0.7 and 1.0).

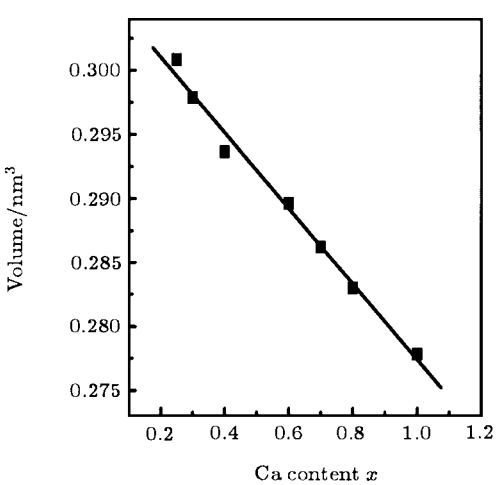


Fig.2. The variation of cell volume with Ca content x.

The XRD study indicates that all the samples are of single phase with a $Sr_3Ti_2O_7$-type tetragonal structure ($I4/mmm$). Figure 1 shows the XRD patterns of the samples $La_{2-2x}Sr_1Ca_{2x}Mn_2O_7$ (x=0.3, 0.5, 0.7 and 1.0). We can clearly see that the XRD peaks change gradually with the increase of the Ca doping content. For example, the positions of the peaks indexed as (105) and (110) gradually shift together toward the high-angle direction. Figure 2 shows a decrease in the values of the cell volume. These observations indicate that the cell volume contracts with the increases of Ca^{2+} ion content x.

The structural parameters of some samples are refined by the Rietveld technique. Figure 3 shows the experimental and calculated XRD patterns for the x=0.6 sample, indicating a good fit. The results of crystal structure refinement are shown in Table 1 for the samples of x=0.3, 0.4, 0.5 and 0.6.

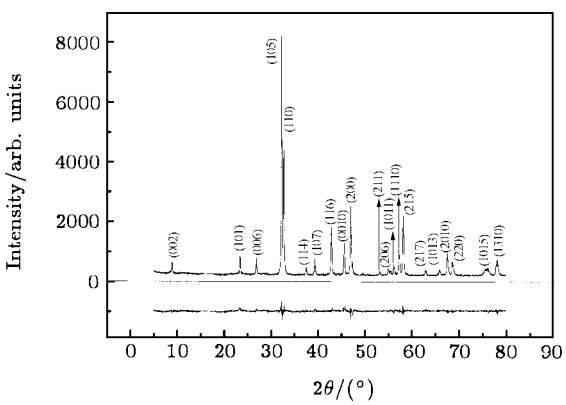


Fig.3. XRD pattern of the $La_{0.8}Sr_1Ca_{1.2}Mn_2O_7$, where crosses indicate the experimental data and the calculated profile is the continuous line overlying these. The lowest curve shows the difference between experimental and calculated patterns.

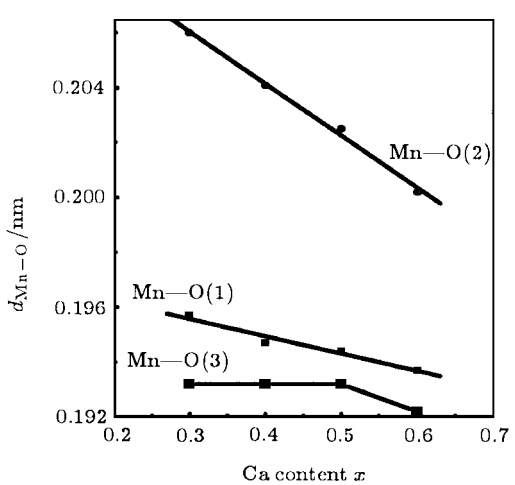


Fig.4. The variation of Mn–O bond lengths in $La_{2-2x}Sr_1Ca_{2x}Mn_2O_7$ with Ca content x at room temperature.

Table 1. The results of crystal structure refinement for all samples. R.WP and R.P denote the weighted pattern R-factor and pattern R-factor, respectively.

x	0.3	0.4	0.5	0.6
a/nm	0.386248(14)	0.386290(17)	0.386329(13)	0.384333(15)
c/nm	1.99242(8)	1.96789(11)	1.97384(7)	1.96083(6.7)
Mn	(0, 0, 0.0982(15))	(0, 0, 0.0989(13))	(0, 0, 0.0987(13))	(0, 0, 0.0988(11))
O(1)	(0, 0, 0)	(0, 0, 0)	(0, 0, 0)	(0, 0, 0)
O(2)	(0, 0, 0.2016(46))	(0, 0, 0.2026(36))	(0, 0, 0.2014(32))	(0, 0, 0.2009(28))
O(3)	(0,0.5, 0.0980(32))	(0,0.5, 0.0975(28))	(0,0.5, 0.0985(28))	(0,0.5, 0.0964(24))
$d_{\mathrm{Mn-O(1)}}$/nm	0.1957(29)	0.1947(2)	0.1944(25)	0.1937(21)
$d_{\mathrm{Mn-O(2)}}$/nm	0.2060(18)	0.2041(7)	0.2025(18)	0.2002(15)
$d_{\mathrm{Mn-O(3)}}$/nm	0.1932(0)	0.1932(0)	0.1932(0)	0.1922(0)
$\theta_{\mathrm{Mn-O(3)-Mn}}$/(°)	179.77	178.34	179.89	177.19
Occu of La (P)	0.652	0.542	0.488	0.408
Occu of Sr/Ca (P)	0.348	0.458	0.512	0.592
Occu of La(P)	0.374	0.329	0.256	0.196
Occu of Sr/Ca(R)	0.626	0.671	0.744	0.804
R.WP	8.34	8.32	8.92	8.92
R.P	6.83	6.44	6.70	6.85

In Fig.4 we find that with the increasing content x of Ca^{2+} ions, the apical Mn–O(1) and Mn–O(2) bond lengths decrease, while the equator Mn–O(3) bond length remains unchanged until x=0.6. Meanwhile the Mn–O–Mn bond angles remain almost unchanged. This is unlike $La_{1.4}(Sr_{1-x}Ca_x)_{1.6}Mn_2O_7$, in which the Mn–O(1) bond length decreases while the Mn–O(2) and Mn–O(3) bond lengths increase with the increase of the Ca doping content.[9]

It is obvious that the change of composition and structure in the compound will affect the interlayer exchange interaction and lead to the change of magnetic properties.

B. Magnetic property

The temperature dependence of magnetization for $La_{2-2x}Sr_1Ca_{2x}Mn_2O_7$ is shown in Fig.5. We can see apparent changes taking place as x increases to 0.4. At x=0.25 and 0.30, we can still observe a long-range magnetic order transition at values of T_C at about 40 and 50K, and another upper transition at 200 and 225K (designated as T^*) which has been ascribed to the short-range or two-dimensional magnetic ordering due to the layered structure, respectively. At $0.30< x <0.80$, the long-range magnetic order disappears but the two-dimensional magnetic order still remains. When the Ca^{2+} content increases, T^* shifts towards a higher temperature. With further doping above x=0.80 and 1.00, no magnetic transition occurs. The field dependence of magnetization at 5K for $La_{2-2x}Sr_1Ca_{2x}Mn_2O_7$ is plotted in Fig.6(a). The M values of all the samples increase linearly as the field increases above 1T and no saturation is reached, even at 5T.

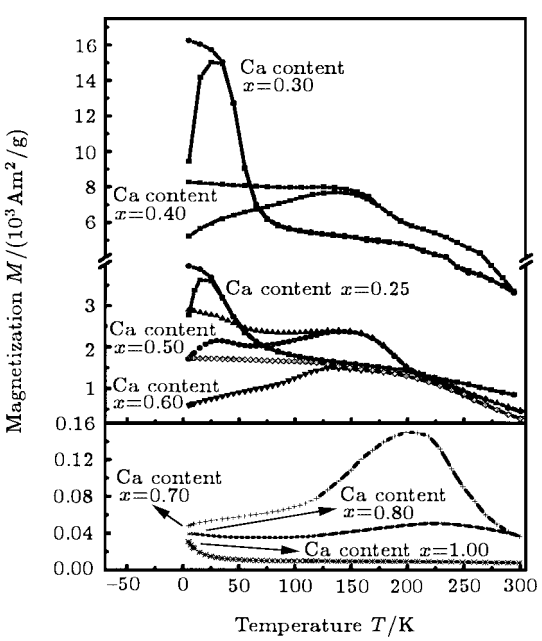


Fig.5. The temperature dependence of magnetization for $La_{2-2x}Sr_1Ca_{2x}Mn_2O_7$, where the measuring field is 0.05T.

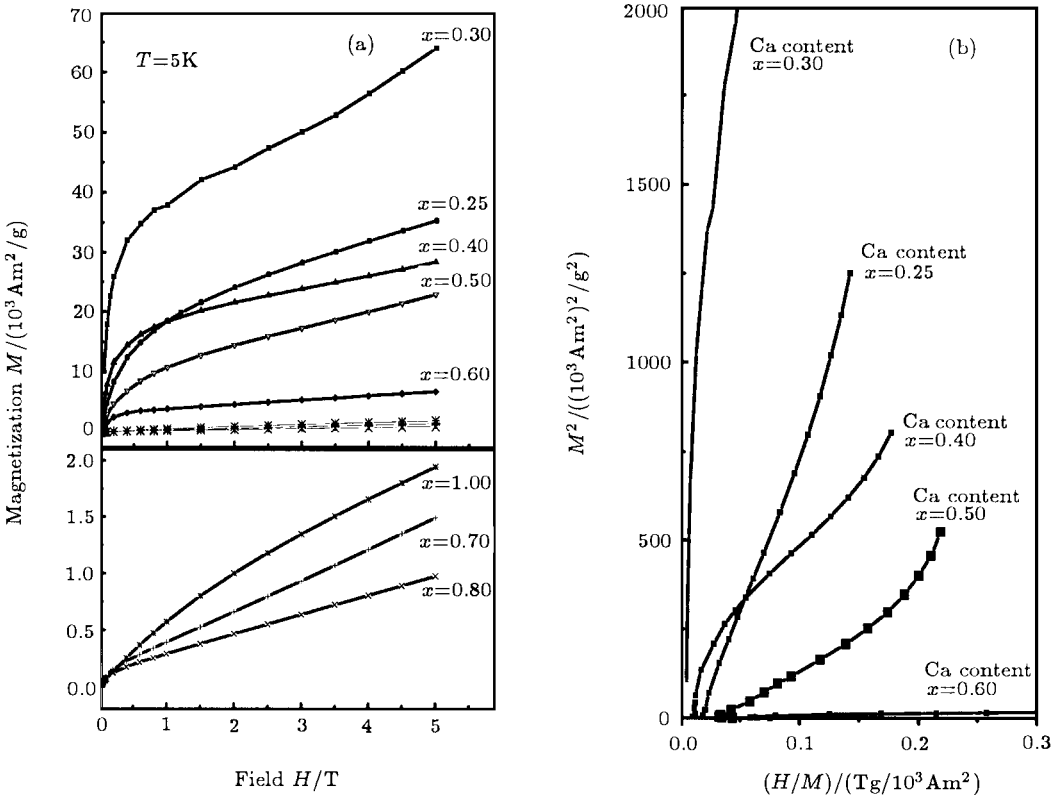


Fig.6. (a) The field dependence of magnetization at 5K for $La_{2-2x}Sr_1Ca_{2x}Mn_2O_7$. (b) Arrot plot of $La_{2-2x}Sr_1Ca_{2x}Mn_2O_7$.

These variations of magnetization, which depend on the doping concentrations, can be considered as a competition of the FM and AFM interactions. In the case of x=0.25, the Mn^{3+}/Mn^{4+} ratio deviates from the ideal value, and thus its T_C and magnetic moment are smaller than those of $La_{2-2x}Sr_1Ca_{2x}Mn_2O_7$ with x=0.30. The large change in the magnetic properties in the high-x range could be ascribed to the contribution of the AFM interaction between Mn^{4+} cations. The hole-doping procedure significantly suppresses the FM state and a spin-canting state or a weak AFM state occurs. The Arrot plot (Fig.6(b)) shows that all the samples have no spontaneous magnetization, and the shape of the M-H curves indicates a canted spin AFM state.

Furthermore, the magnetic measurement indicates that the samples exhibit spin-glass-like behaviour instead of ferromagnetism at low temperatures. For example, when x=0.30, after zero-field-cooling (ZFC) and field-cooling (FC) from room temperature to 5K, the M against temperature T curves were measured in the fields of 0.05, 1.00 and 5.00T; the results are shown in Fig.7. A sharp cusp is observed in the ZFC data at about 30K when the applied field is just 0.05T, but this cusp loses its sharpness with increasing external field until 5.00T. In Fig.7, one can note that the FC curves remain to coincide with the ZFC curves at high temperatures until they reach the cusp of the ZFC curves. But, below the temperature of the cusp of the ZFC curves, they begin to deviate from the ZFC traces, and the deviation increases gradually as temperature decreases. The magnetic behaviour is dependent on whether the samples are cooled down with or without an applied field. This is a characteristic of spin glasses.[11]

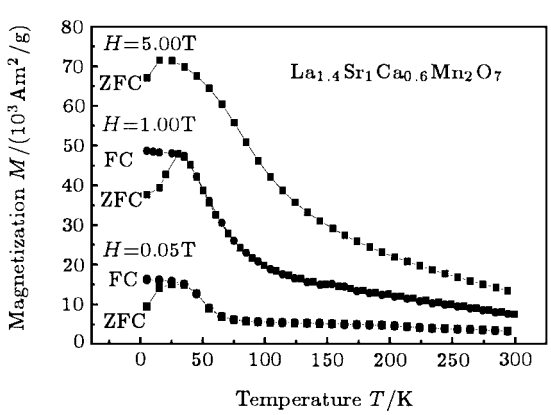


Fig.7. Magnetization versus temperature $M(T)$ for ZFC (solid squares) and FC (solid circles) processes in the fields of 0.05, 1.00 and 5.00T.

As mentioned above, in addition to the competition of the FM and AFM interactions due to the change of the Mn^{3+}/Mn^{4+} ratio, the Jahn–Teller-type lattice distortion of MnO_6 octahedra plays an important role. The structure refinement results in Table 1 show that the substitution of La by Ca results in the changes of Mn–O bond length, and the total effects contributed by the changes of Mn–O(2), Mn–O(1) and Mn–O(3) bonds lead to the reduction of the exchange interaction between bilayers and intralayer Mn ions. This results in the disappearance of three-dimensional spin ordering, the appearance of the canted AFM ordering and clusters of spin-glass arrangement along with the increase of Ca^{2+} content x.

IV. CONCLUSIONS

The substitution of Ca for La in $La_{2-2x}Sr_1Ca_{2x}Mn_2O_7$ results in the weakening and then the disappearance of long-range FM ordering, the formation of spin canting, antiferromagnetic ordering and low-temperature spin-glass. These variations of magnetic properties are related to a competition of the FM and AFM interactions, resulting from the change of the Mn^{3+}/Mn^{4+} ratio and Jahn–Teller-type lattice distortion of MnO_6 octahedra due to the introduction of Ca^{2+} ions.

References

[1] Mitchell J F, Argyriou D N, Jorgensen J D, Hinks D G, Potter C D and Bader S D 1997 *Phys. Rev.* B **55** 63

[2] Argyriou D N, Mitchell J F, Potter C D, Bader S D, Kleb R and Jorgensen J D 1997 *Phys. Rev.* B **55** 11 965

[3] Battle P D, Cox D E, Green M A, Millburn J E, Spring L E, Radaeli P G, Rosseinsky M J and Vente J F 1997 *Chem. Mater.* **9** 1042

[4] Moritomo Y, Asamitsu A, Kuwahara H and Tokura Y 1996 *Nature* **380** 141

[5] Kimura T, Tomioka Y, Kuwahara H, Asamitsu A, Tamura M and Tokura Y 1996 *Science* **274** 1698

[6] Seshadri P, Maignan A, Hervieu M, Nguyen N and Raveau B 1997 *Solid State Commun.* **101** 453

[7] Zener C 1951 *Phys. Rev.* **81** 440
Zener C 1951 *Phys. Rev.* **82** 403

[8] Millis A J, Littlewood P B and Shraiman B I 1995 *Phys. Rev. Lett.* **74** 5144
Millis A J *et al* 1996 *Phys. Rev. Lett.* **77** 175

[9] Chang C F, Chou P H, Tsay H L, Wng S S, Chatterjee S, Yang H D, Liu R S, Shen C H and Li W H 1998 *Phys. Rev.* B **58** 12 224

[10] Ganguly R, Siruguri V, Gopalakrishnan I K and Yakhmi J V 2000 *J. Phys.: Condens. Matter* **12** 1683

[11] Cai J W, Wang C, Shen B G, Zhao J G and Zhan W S 1997 *Appl. Phys. Lett.* **71** 1727